SLAC-PUB-10039
KEK-PREPRINT-93-190

Beam-Beam Interaction with a Crossing Angle[1]

Kohji Hirata

KEK, National Laboratory for High Energy Physics
and Stanford Linear Accelerator Center

A fairy accurate mapping for the beam-beam interaction with a crossing angle is proposed. Some simple results of the weak-strong tracking are shown: the beam-beam interaction becomes more serious when the crossing angle increases until the normalized angle Φ becomes about a half. Above this, it becomes less serious. When $\Phi \gtrsim 1$, the beam size becomes almost unaffected.

1 Introduction

It seems widely believed that the beam-beam effects become more serious for larger crossing angle. Is it in the world true? To confirm it, we need the followings:

1. An **accurate** model of the interaction; it may not be **exact** but we should use the most accurate mapping possible. All previous theoretical works have relied on the famous paper of Piwinski[1]. His mapping would be right if the bunch-length effect can be ignored. We will propose more convincing mapping.

2. A **reliable** simulation; As E. Keil[2] talked, *In order to simulate a phenomenon well all relevant dynamic processes must be included. Since it is* **a priori** *not known which processes are relevant, all of them must be included.* I think it true. Of course, **inclusion** of many processes alone does not automatically imply the result is reliable: each process should be treated in a right way. From this point of view, this paper is not sufficient because we consider the Hamiltonian beam-beam mapping alone and we exclude all other dynamical processes like wake field or nonlinear optical effects. Our method, however, can be extended to such cases because our beam-beam mapping is **local**[3].

3. A **clear** experiment; For small crossing angle, there are several experiments but that at DORIS[1] was the only one with a large angle. The next generation high-luminosity meson factories will provide good data for a large crossing angle if one of them will employ it.

The principal aim of this paper is to propose a new mapping for the beam-beam interaction (in the next section) which I believe is the most accurate we have ever had.

2 Beam-Beam Mapping

Here, we present the beam-beam mapping for the collision with a crossing angle. It is the best in existing mappings in that

♡ It is symplectic in 6-dimensional sense.

♡ It includes all the known effects and some new effects.

[1]Work partly supported by Department of Energy contract DE-AC03-76SF00515.

Submitted to the 6th Advancd ICFA Beam Dynamics Workshop,
Funchal, Madeira, 24-30 Oct 1993.

Stanford Linear Accelerator Center, Stanford University, Stanford, CA 94309, USA

♡ It is **local**. That is, it is to be applied at one point in a ring (called $s = 0$) and therefore it can be used regardless to the other part of the ring.

The basic idea is as follows:

◇ We divide the difficulty of treating complicated geometry of colliding beams in an angle into two pieces. We apply the Lorentz boost[4, 5] to make the collision head-on. The beam-beam kick is evaluated in a Lorentz frame in which the collision appears to be head-on but they are tilted horizontally.

◇ For the head-on collision, we use the mapping, called the synchro-beam mapping (SBM). This is formulated only for the head-on collision[6]. This includes implicitly the effects of the electric field and the hourglass effects[7]. The bunches are cut into many pieces longitudinally. We apply the SBM for pairs of these slices.

◇ The Lorentz transformation is symplectic[5] and will be treated in an exact manner within the ultrarelativistic approximation. Thanks to the 6-dimensional nature of the SBM, it is relatively easy.

The idea may be read off from Fig.1.

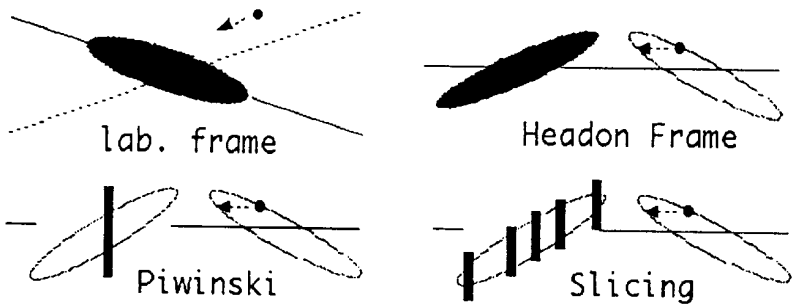

Figure 1: Longitudinal slicing is necessary for the collision with a crossing angle. At each slice, the electric field effect does not cancel and should not be ignored.

Let us assume one IP in a ring ($s = 0$). At the IP, coordinates are boosted so that the collision becomes head-on ($\mathcal{L}$). Then it interacts with the other beam in this boosted frame where the SBM is used. The particle is then transformed back to the original frame ($\mathcal{L}^{-1}$). It is transformed from IP to IP by some appropriate mapping ($\mathcal{A}$) as is done in the particle tracking codes. We denote the variables of each step as follows:

$$\boldsymbol{x}(0)\xrightarrow{\mathcal{L}}\boldsymbol{x}^*(0^*)\xrightarrow{\mathrm{SBM}}\boldsymbol{x}^{*\prime}(0^*)\xrightarrow{\mathcal{L}^{-1}}\boldsymbol{x}'(0)\xrightarrow{\mathcal{A}}\boldsymbol{x}(0)\cdots.$$

We always transform quantities at $s = 0$ to those at $s = 0$.

We employ the coordinate system: $\boldsymbol{x} = (x, p_x, y, p_y, z, p_z; h, s)$. Here x and y are horizontal and vertical coordinates and their conjugate momenta are defined as

$$(p_x, p_y) = m\gamma(dx/ds, dy/ds)/P_0,$$

where P_0 is the absolute value of the three-momentum $\boldsymbol{P}$ of the reference particle, m the mass of the electron and γ the relativistic Lorentz factor. We use $z = s - ct(s)$, where c is the light velocity, t the arrival time to the position s and $p_z = (|\boldsymbol{P}| - P_0)/P_0$. The h is the "Hamiltonian": we use

$$h(p_x, p_y, p_z) = p_z + 1 - \sqrt{(p_z+1)^2 - p_x^2 - p_y^2}. \tag{1}$$

This is the momentum along the reference trajectory and s is the "time" which is the position in the ring. Here the ultra-relativistic limit is taken.

Lorentz Boost It can be shown[8] that the Lorentz boost ($\mathcal{L}$) can be put in a form

$$\begin{aligned} x^* &= \tan\phi z + [1 + h_x^* \sin\phi]x \\ y^* &= y + \sin\phi h_y^* x \\ z^* &= z/\cos\phi + h_z^* \sin\phi x \\ p_x^* &= (p_x - \tan\phi h)/\cos\phi \\ p_y^* &= p_y/\cos\phi \\ p_z^* &= p_z - \tan\phi p_x + \tan^2\phi h. \end{aligned}$$

This map is quasi-symplectic: the Jacobian of the transformation is $1/\cos^3\phi$. It is due to the fact that we are using the normalized momentum (and P_0 changes under the boost) but is not a problem at all because the inverse factor is applied by $\mathcal{L}^{-1}$.

Beam-Beam Force: SBM The strong beam is cut into slices: each slice is represented by its $z^*(0^*)$ coordinate, denoted by $z^\dagger$. (We put $\dagger$ for quantities of the strong beam at $s^* = 0$.) We get $\sigma_z^\dagger = \sigma_z/\cos\phi$. The first and second moments of slices are (a linear approximation is used)

$$X^\dagger = \sin\phi z^\dagger, \qquad Y^\dagger = 0, \qquad P_x^\dagger = 0, \qquad P_y^\dagger = 0, \qquad P_z^\dagger = 0,$$

$$\Sigma_{11}^\dagger = \Sigma_{11}, \qquad \Sigma_{22}^\dagger = \Sigma_{22}/\cos^2\phi, \qquad \Sigma_{33}^\dagger = \Sigma_{33}, \qquad \Sigma_{44}^\dagger = \Sigma_{44}/\cos^2\phi.$$

The SBM is presented in detail in Ref.[6]. It can be represented by a Hamiltonian $H = H_{bb}(\boldsymbol{x}^*)\delta(s^*)$, where H_{bb} is defined implicitly by

$$\exp : H_{bb} := \prod_{z^\dagger} \exp : F(\boldsymbol{x}^*, z^\dagger) : .$$

Here $F(\boldsymbol{x}^*, z^\dagger)$ describes the interaction with a slice having $z^\dagger$. It is applied such that a particle collides first with the slice with the largest $z^\dagger$ and then with the next largest and so on. Here

$$F(\boldsymbol{x}^*; z^\dagger) = n^* U\Big(X^*, Y^*; \Sigma_{11}^\dagger(S), \Sigma_{33}^\dagger(S)\Big),$$

where n^* is the number of particles in the slice, $S = S(z^*, z^\dagger) = (z^* - z^\dagger)/2$ is the value of s^* for the real collision, $X^* = x^* + p_x^* S - X^\dagger(z^\dagger)$ and $Y^* = y^* + p_y^* S - Y^\dagger(z^\dagger)$. We assume transverse distribution of each slice is Gaussian so that

$$U(x, y; \Sigma_{11}, \Sigma_{33}) = -\frac{r_e}{\gamma_0} \int_0^\infty \frac{\exp\left(-\dfrac{x^2}{2\Sigma_{11} + u} - \dfrac{y^2}{2\Sigma_{33} + u}\right)}{\sqrt{2\Sigma_{11} + u}\,\sqrt{2\Sigma_{33} + u}}\, du.$$

In a simulation, the longitudinal slices are made in such a way that all slices represent the same number of particles[6].

Note that we have employed the Gaussian approximation in evaluating U. This cannot be justified for the strong-strong case. In other words, the weak-strong picture should not be used for large value of the current. In fact, it was once criticized by Krishnagopal and Siemann[9]. They found a new effect when they avoided this approximation. Later, however, Krishnagopal and Chin[10] have pointed out that the same effect can occur with the Gaussian approximation if one kills the barycentre motions. Also in one dimensional simulation[11], there does not seem to exist any remarkable difference between cases with and without using this approximation for the equilibrium states.

3 Simulation

The analysis of the head-on collision[12] has shown that the synchro-betatron resonances are weakened by the bunch length effect. (This was not sufficiently satisfactory because they have ignored the effect on the longitudinal degree of freedom but this result is true because the same effect was seen in a simulation in which the SB mapping was applied.) Why don't we expect the same thing for the case with a crossing angle.

To see the effects of the beam-beam interaction with a crossing angle, we will try a weak-strong simulation. To fix the model, we should tell how we treat the arc, i.e., from IP to IP.

Arc: $\mathcal{A}$ We use a simple mapping for the arc ($\mathcal{A}$). A coordinate $\boldsymbol{x}$ is transformed first as $\boldsymbol{x} \to diag(U_x, U_y, U_z)\boldsymbol{x}$, where

$$U_{x,y} = \lambda_{x,y}\begin{pmatrix} \cos\mu_{x,y} & \beta^0_{x,y}\sin\mu_{x,y} \\ -\sin\mu_{x,y}/\beta^0_{x,y} & \cos\mu_{x,y}\end{pmatrix}, U_z = \begin{pmatrix} \cos\mu_z & -\beta^0_z\sin\mu_z \\ \lambda_z^2\sin\mu_z/\beta^0_z & \lambda_z^2\cos\mu_z\end{pmatrix}.$$

with $\lambda_{x,y,z} = \exp(-1/T_{x,y,z})$. Here T's are damping turns. Then we apply

$$x \to x + \sigma^0_x\sqrt{1-\lambda_x^2}\hat{r}_1, \qquad p_x \to p_x + \sigma^0_{p_x}\sqrt{1-\lambda_x^2}\hat{r}_2,$$

$$y \to y + \sigma^0_y\sqrt{1-\lambda_y^2}\hat{r}_3, \qquad p_y \to p_y + \sigma^0_{p_y}\sqrt{1-\lambda_y^2}\hat{r}_4,$$

$$p_z \to p_z + \sigma^0_z\sqrt{1-\lambda_z^4}\hat{r}_5,$$

where $\hat{r}$'s are the standard Gaussian random variables.

The above treatment of the radiation is not exact but the most suitable for a ring with large transverse tunes and a small synchrotron tune[13]. We can add effects of α's and dispersions easily.

Model We use a reasonable set of parameters listed in Tab. 1. We track 50 particles for 10000 turns and accumulate data for beam sizes and the largest amplitudes. Usually, 5 slices are enough.

emittances	(ϵ_x, ϵ_y)	$(2\times10^{-8}, 2\times10^{-10})$ m
betatron functions at IP	(β^0_x, β^0_y)	$(1, 0.01)$ m
bunch length and energy spread	$\sigma_z, \sigma_\epsilon$	$(0.01\text{m}, 1\times10^{-3})$
tunes	(ν_x, ν_y, ν_z)	(0.2,0.15,0.08)
damping turns	T_x, T_y, T_z	2000,2000,1000

Table 1: Standard parameters.

Weak-Current For a small value of the nominal beam-beam parameter, $\eta_{x,y} = 0.01$, the beam sizes are shown in Fig.2.

For $\phi = 0$, the peaks indicate the resonances (from left to right) $n(\nu_x - \eta_x/2) + m(\nu_y - \eta_y/2) + l\nu_z =$ integer for $(n,m,l) = (0,2,-1), (0,2,-2), (2,-2,-1), (2,-2,0), (0,4,0), (2,2,0), (2,2,-1), (0,2,2), (0,2,1)$ and $(0,2,0)$. For $\phi = 5$mrad, major difference is only that $(1,2,0)$ and $(1,-2,0)$ appear. The latter two resonances are not the SB resonances and are stronger for larger ϕ. These were induced by the nonlinear terms in $\mathcal{L}$ and $\mathcal{L}^{-1}$.

Figure 2: (a) The σ_y/σ_y^0 (solid) and σ_x/σ_x^0 (dotted) for $\phi = 0$. (b) the same for $\phi = 5$ mrad. The $\eta = 0.01$.

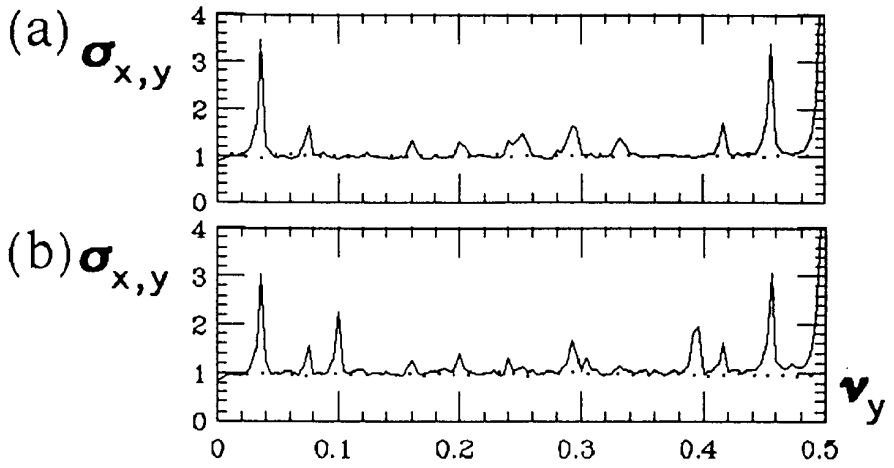

Strong Current Let us put $\eta_{x,y} = 0.05$ and compare several values of ϕ. See Figs.3 and 4. It appears that the effect of ϕ on σ's (Fig.3 and Fig.4-a) and amplitudes (Fig.4-b) increases with ϕ first but becomes to decrease for larger ϕ. This is quite contrary to what is expected from Piwinski's formalism.

Figure 3: The σ_y/σ_y^0 (solid) and σ_x/σ_x^0 (dotted) for (a) $\phi = 0$, (b) $\phi = 5$ mrad and (c) $\phi = 20$ mrad. The $\eta = 0.05$.

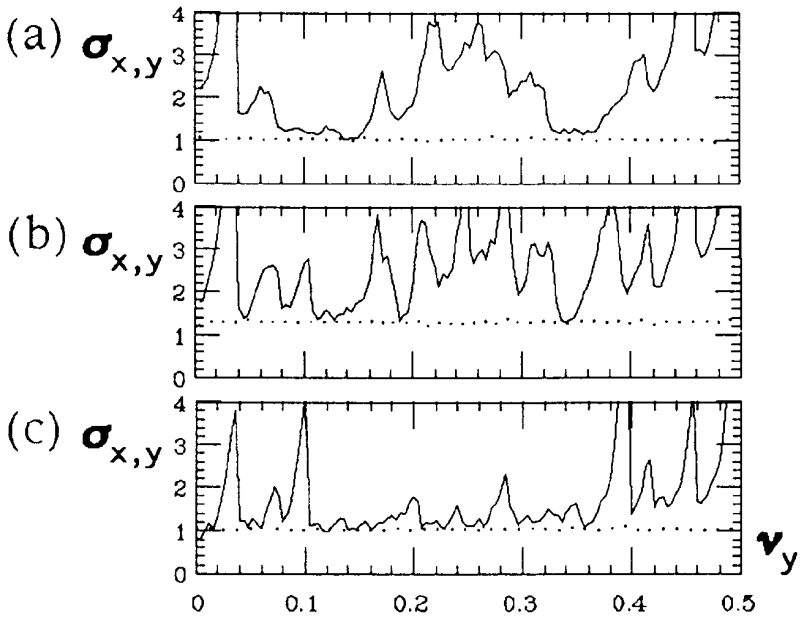

4 Discussion

Effective beam-beam force. It seems useful to consider the luminosity L and effective beam-beam parameter ξ in the boosted frame. Including the hourglass[7] and the beam tilt effects, but excluding the dynamical effects, we define R_L (luminosity reduction factor) and R_ξ (beam-beam reduction factor):

$$R_L = \frac{L}{L_0} = \sqrt{\frac{2}{\pi}} a e^b K_0(b), \tag{2}$$

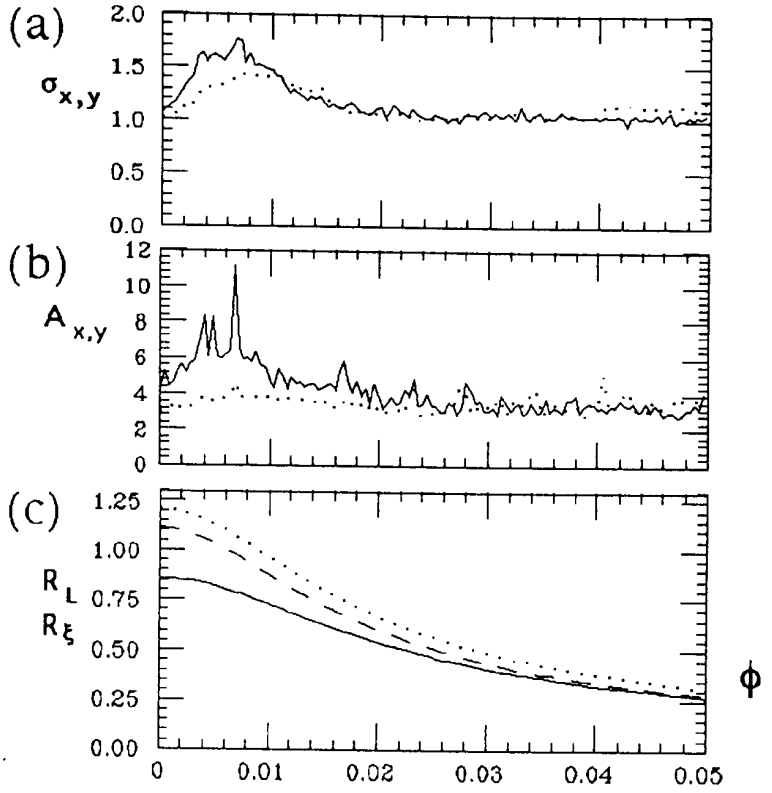

Figure 4: The ϕ dependence. (a) The σ_y/σ_y^0 (solid) and σ_x/σ_x^0 (dotted). (b) The A_x (solid) and A_y (dotted), the horizontal and vertical maximum amplitudes normalized by $\sigma_{x,y}^0$. (c) The luminosity reduction factor R_L (solid), the ξ reduction factor for $z = 0$ particle (dashed) and the same for $z = \sigma_z$ particle(dotted).

$$a = \frac{\sigma_y^*}{\sqrt{2}\sigma_z^*\sigma_{p_y}^*}, \qquad b = a^2\left[1 + \left(\frac{\sigma_z^*}{\sigma_x^*}\tan\phi\right)^2\right],$$

$$R_\xi = \frac{\xi}{\eta} = \int dz^\dagger \rho(z^\dagger)\sqrt{1 + (S/\beta_y^0)^2}F_y(z^\dagger\tan\phi, \sigma_x^*(S), \sigma_y^*(S)), \tag{3}$$

where L_0 is the luminosity without hourglass nor tilt effect, K_0 a Bessel function and $F_y(x, \sigma_x, \sigma_y)$ is Montague's reduction factor[14] of ξ for an off center particle, which falls down with ϕ quite rapidly. These are shown in Fig.4-c. For small ϕ, R_ξ is even larger than 1 due to the hourglass effect which makes the beam-beam interaction more serious. This decreases rapidly for larger ϕ. At the same time, R_L also decreases but less rapidly.

Importance of using slices The essential difference from Piwinski's formalism is the inclusion of the bunch length effect by using several slices. In fact, if we use only one slice, the effect grows almost proportional to ϕ and does not begin to decrease. From Eqs.(2) and (3), it seems that two parameters are important: $R = \sigma_z/\beta_y^0$ and $\Phi = \phi\sigma_z/\sigma_x$. For $R \gtrsim 1$, the hourglass effect is important even for $\phi = 0$ [12]. When $\Phi \gtrsim 1$ the tilt effect is important. Piwinski's formalism worked well for DORIS where $R \ll 1$ and $\Phi \simeq 1/2$ (DORIS used vertical crossing so that σ_x is to be replaced by σ_y in Φ). In Piwinski's formalism, R_ξ and R_L decrease in the same manner.

Speculation When $\phi > 0$, compared to $\phi = 0$ case, R_L is smaller, but R_ξ is even smaller so that it is reasonable that the beam blowup is less serious. Since L is proportional to $1/(\sigma_x\sigma_y)$, it has a second maximum at some $\phi \neq 0$.

In the present example, as a function of ϕ, we have

ϕ	σ_x	σ_y	R_L	L/L(0)
0	1	1	0.86	0.86
7	1.4	1.8	0.78	0.31
10	1.4	1.5	0.72	0.34
15	1.2	1.1	0.63	0.48
16	1.1	1.1	0.61	0.50
20	1	1.1	0.54	0.49

The largest amplitudes fall off also for larger ϕ. Within the parameter region so far surveyed, it seems that R_L has the second peak at $\Phi \simeq 1$. The value of R_L at this angle differs for different R.

Implication Large ϕ has several merits for high luminosity rings; 1) Luminosity reduction is only geometrical origin. 2) If we use the crab crossing[15], in addition, the geometrical reduction of the luminosity might be recovered. Even without it, the loss of the luminosity is not fatal; 3) More bunches can be used: the luminosity is also proportional to N_b, the number of bunches in a beam. Larger ϕ allows more N_b[16]. If ϕ is larger than a few radians, N_b can be as large as the harmonic number. This enhances the luminosity. 4) From Fig.3, the good region in the tune space is much wider.

Shorter Bunch The rate of fall-off of the beam size with ϕ depends a little on the tunes. On some resonances, in particular, the beam sizes remain large. These points can be avoided easily. For shorter bunches, the first merit becomes less remarkable but still exists. For $\sigma_z = \beta_y^0/2$ with the other parameters being unchanged, for an example, the maximum occurs at around $\phi = 40$ mrad and it gives $L/L_0 = 56\%$.

ϕ	σ_x	σ_y	R_L	L/L(0)
0	1	1	0.95	0.95
10	1.3	1.3	0.89	0.53
20	1.4	1.3	0.78	0.43
30	1.2	1.1	0.67	0.51
40	1.0	1.0	0.56	0.56

The author wishes to thank M. Furman, H. Moshammer, R. Siemann and K. Oide for valueable discussions. He also thanks the members of the group of R. Ruth at SLAC for their hospitality extended to him.

References

[1] A. Piwinski, DESY Report DESY 77/18 (1977).

[2] E. Keil, AIP Conf. Proc. **105**, 651 (1982).

[3] É. Forest and K. Hirata, *A Contemporary Guide to Beam Dynamics*, KEK Report 92-12 (1992).

[4] J. Augustin, Orsay, 36-69 (1969).

[5] K. Oide, private communication (1990).

[6] K. Hirata, H. Moshammer and F. Ruggiero, Part. Accel. 40, 205 (1993).

[7] G. E. Fischer, SLAC report SPEAR-154 (1972). SPEAR Storage Ring Group, IEEE Trans. Nucl. Sci. **NS-20**, 3, 838 (1973). M. Furman, Proc. 1991 IEEE Particle Accelerator Conference p.422 (1991).

[8] K. Hirata, SLAC report SLAC-PUB-6375 (1993).
[9] S. Krishnagopal and R. Siemann, Phys. Rev. Lett. **67**, 2461 (1991).
[10] S. Krishnagopal and Y. H. Chin, B factories", SLAC-400 (1992).
[11] K. Hirata and S. Matsumoto, KEK Preprint 93-24 (1993).
[12] Krishnagopal and Sieman, Phys. Rev. **D41**, 2312 (1990).
[13] K. Hirata and F. Ruggiero, Part. Accel. **28**, 137 (1990).
[14] B. W. Montague, CERN report CERN/ISR-GS/75-36 (1975).
[15] K. Oide and K. Yokoya, Phys. Rev. A **40**, 315 (1989).
[16] K. Hirata, AIP Conference Proceedings No.214, Ed. A.M.Sessler, p.441 (1990). K. Hirata, KEK report, KEK Proceedings 93-7, p.84 (1993).